A sequential model for disaggregating near-surface soil moisture observations using multi-resolution thermal sensors

Olivier Merlin, Al Bitar Ahmad, J P. Walker, Yann H. Kerr

HAL Id: ird-00403130
https://ird.hal.science/ird-00403130

A sequential model for disaggregating near-surface soil moisture observations using multi-resolution thermal sensors

Olivier Merlin [a,*], Ahmad Al Bitar [a], Jeffrey P. Walker [b], Yann Kerr [a]

[a] Centre d'Etudes Spatiales de la Biosphère (CESBIO), Toulouse, France
[b] Civil and Environmental Engineering, The University of Melbourne, Australia

ABSTRACT

A sequential model is developed to disaggregate microwave-derived soil moisture from 40 km to 4 km resolution using MODIS (Moderate Imaging Spectroradiometer) data and subsequently from 4 km to 500 m resolution using ASTER (Advanced Scanning Thermal Emission and Reflection Radiometer) data. The 1 km resolution airborne data collected during the three-week National Airborne Field Experiment 2006 (NAFE'06) are used to simulate the 40 km pixels, and a thermal-based disaggregation algorithm is applied using 1 km resolution MODIS and 100 m resolution ASTER data. The downscaled soil moisture data are subsequently evaluated using a combination of airborne and in situ soil moisture measurements. A key step in the procedure is to identify an optimal downscaling resolution in terms of disaggregation accuracy and sub-pixel soil moisture variability. Very consistent optimal downscaling resolutions are obtained for MODIS aboard Terra, MODIS aboard Aqua and ASTER, which are 4 to 5 times the thermal sensor resolution. The root mean square error between the 500 m resolution sequentially disaggregated and ground-measured soil moisture is 0.062 vol./vol. with a bias of −0.045 vol./vol. and values ranging from 0.08 to 0.40 vol./vol.

© 2009 Elsevier Inc. All rights reserved.

1. Introduction

Predicting the spatio-temporal variability of hydrological processes requires models that operate at different scales: evapotranspiration and infiltration at paddock-scale, run-off and drainage at catchment-scale, and atmospheric circulation at meso-scale. Due to the complexity of interacting processes (Chehbouni et al., 2008), the reliability of model predictions is intimately related to the ability to represent dominant processes in space and time using observations. Remote sensing has shown promise for this application due to its multi-resolution and multi-spectral capabilities (Choudhury, 1994).

Among the variables observable from space, soil moisture is one of the most crucial parameters that control hydrometeorological processes from paddock- to meso-scale. However, current and near-future space-borne soil moisture products have a spatial resolution of several tens of kilometers (Crow et al., 2005) —about ~40 km resolution for the forthcoming Soil Moisture and Ocean Salinity (SMOS, Kerr et al., 2001) mission—, which make their application to hydrological and agricultural models challenging.

Downscaling methodologies are therefore needed to improve the spatial resolution of passive microwave-derived soil moisture. To understand how soil moisture scales, the spatial structure of soil moisture fields has been statistically described using experimental data sets aggregated at a range of resolutions. Those studies (e.g. Rodriguez-Iturbe et al., 1995; Das & Mohanty, 2008) conducted over different sites and using either remotely sensed or ground-based data, conclude that soil moisture behaves as a fractal —i.e. follows a power law decay— over a wide range of scales. Moreover, there is a general agreement that the fractal behaviour of soil moisture is not simple over extended scale ranges, and changes in time (Kim & Barros, 2002b; Dubayah et al., 1997; Western et al., 2002). In particular, the recent study of Das and Mohanty (2008) suggests a transition from simple fractal (in wet fields) to multi-fractal (in dry fields) behaviour during a dry-down period. In practice, the multi-fractal framework seems an appropriate basis for downscaling soil moisture fields in areas where ancillary data (e.g. topography, soil properties, vegetation, rainfall) are available at high resolution (Kim & Barros, 2002a).

One drawback with statistical approaches is that they require a large amount of data given that their validity domain is generally limited to the conditions used for calibration. Consequently, there is a need to develop methods that use physical and observable parameters. Bindlish and Barros (2002) developed an interpolation method to downscale L-band passive microwave data using active microwave data at the same wavelength to improve the resolution of

Q1 * Corresponding author.
E-mail address: olivier.merlin@cesbio.cnes.fr (O. Merlin).

brightness temperature fields prior to soil moisture retrieval. Similarly, Merlin et al. (2008a) developed a deterministic downscaling algorithm that combines 1 km resolution MODIS (MODerate resolution Imaging Spectroradiometer) data and a semi-empirical soil evaporative efficiency model. The main advantage of those approaches (Bindlish & Barros, 2002; Merlin et al., 2008a) over the purely empirical ones based on log–log plots (e.g. Kim & Barros, 2002a) is that some physical considerations are used to build a relationship between soil moisture and an ancillary observable; radar backscatter in Bindlish and Barros (2002) and soil evaporative efficiency in Merlin et al. (2008a).

In Merlin et al. (2008a), the disaggregation scale was fixed to 10 times the spatial resolution of MODIS thermal data to reduce the random uncertainties in disaggregated soil moisture. The authors observed that the sub-pixel variability of disaggregated soil moisture was significantly correlated with the observed fine-scale soil moisture variability, suggesting that the downscaling algorithm could be applied to spatial resolutions finer than 10 km. Nevertheless, that study did not apply the downscaling approach at multiple resolutions.

As a follow-up of Merlin et al. (2008a), this paper seeks to identify optimal downscaling resolutions in terms of disaggregation accuracy and sub-pixel spatial variability, and demonstrate the utility of this approach for sequential disaggregation of spaceborne surface soil moisture observations using multi-resolution thermal sensors. The development of a sequential approach is motivated by (i) the fact that high-resolution thermal data such as ASTER (Advanced Scanning Thermal Emission and Reflection Radiometer) data generally have a swath width smaller than the SMOS pixel and (ii) the hypothesis that the use of an intermediate resolution provides a better linearized approximation to a non linear function (e.g. soil evaporative efficiency model). One objective of the paper is to assess this hypothesis using data collected during the three-week National Airborne Field Experiment 2006 (NAFE'06). Airborne L-band data are used to simulate the 40 km resolution pixels expected from SMOS, and a thermal-based disaggregation algorithm is applied using MODIS and ASTER data. While the first part of the paper focuses on estimating optimal downscaling resolutions with MODIS and ASTER data, the second part takes advantage of these results to develop a sequential model for disaggregating ~40 km resolution microwave-derived soil moisture to 500 m.

2. Data

The NAFE'06 was conducted from 31 October to 20 November 2006 over a 40 km by 60 km area near Yanco ($-35°$N; $146°$E) in southeastern Australia. While a full description of the data set is given in Merlin et al. (2008b), a brief overview of the most pertinent details are provided here. The data used in this study are comprised of wind speed measurements, L-band derived soil moisture and MODIS data collected over the Yanco area on twelve days, and ground measurements of 0–5 cm soil moisture and ASTER data collected over three 9 km^2 areas included in the Yanco area on one day (16 November) of the experiment.

2.1. Wind speed

Wind speed was monitored at 2 m by a meteorological station (located in the southwestern corner of the Yanco area, see Fig. 1 of Merlin et al. (2008b)) continuously during NAFE'06 with a time step of 20 min. The time series is illustrated in Fig. 1 of Merlin et al. (2008a).

2.2. Ground soil moisture

In situ measurements of 0–5 cm soil moisture were made using HDAS (Hydraprobe Data Acquisition System) on 16 November over three 9 km^2 sampling areas (denoted as Y2, Y9 and Y12) included in the 40 km by 60 km Yanco area (Merlin et al., 2008b). Within each 9 km^2 sampling area, an average of three successive measurements was made ~1 m apart at each node of a 250 m resolution grid.

2.3. PLMR-derived soil moisture

The near-surface soil moisture was retrieved from the 1 km resolution brightness temperature collected by the Polarimetric L-band Multibeam Radiometer (PLMR) on eleven days over the 40 km by 60 km area: 31 October, 2, 3, 4, 5, 7, 9, 13, 14, 16, 18 November (Merlin et al., 2009). The surface temperature data used for the PLMR soil moisture inversion came from MODIS data on clear sky days, and from in situ measurements on overcast days. The root mean square difference between PLMR-derived and ground-measured soil moisture at 1 km resolution was estimated to 0.03 vol./vol. in non-irrigated areas. A bias of about -0.09 vol./vol. was obtained over pixels including some irrigation. This bias was explained by a difference in sensing depth between the L-band radiometer (~0–3 cm) and in situ measurements (0–5.7 cm), associated with a strong vertical gradient in the top 0–6 cm of the soil. Moreover on 3 November, which followed a rainfall event, the PLMR-derived soil moisture seemed to be affected by the presence of water intercepted by vegetation (Merlin et al., 2008b,a). In this study, data from this date were discarded.

2.4. MODIS data

The MODIS data used in this paper are the Version 5 MODIS/Terra (10:30 am) and MODIS/Aqua (1:30 pm) 1 km resolution daily surface temperature, and MODIS/Terra 250 m resolution 16-day Normalized Difference Vegetation Index (NDVI). The 16-day NDVI product was cloud free. In between the first (31 October) and last day (18 November) of 1 km resolution PLMR flights over the Yanco area, sixteen MODIS Version 5 surface temperature images with 0% cloud cover were acquired including nine aboard Terra (3, 5, 7, 8,9,10, 11, 17,18 November) and seven aboard Aqua (31 October, 3, 4, 6, 8, 9, 17 November). Note that more cloud free images were obtained than from Version 4 surface temperature (Merlin et al., 2008a). The overestimation of cloud cover in Version 4 products and the subsequent increase of coverage in Version 5 land surface temperature products are discussed in Wan (2008). MODIS data were re-sampled on the same 1 km resolution grid as PLMR-derived soil moisture, and MODIS surface temperature was shifted of ($+1$ km E; -0.5 km N) and ($+2$ km E; 0 N) for Terra and Aqua respectively to maximize the spatial correlation with 1 km resolution MODIS NDVI, which was used as a reference for the co-registration.

2.5. ASTER data

The ASTER/Terra overpass of the NAFE'06 site was on 16 November 2006 at 10:30 am. Radiometric surface temperature was estimated from 90 m resolution L1B thermal radiances using the emissivity normalization method developed by Gillespie (1985) and Realmuto (1990) and implemented in ENVI (ENvironment for Visualizing Images, http://www.ittvis.com/envi/) image processing software. Temperature was computed for each of the five thermal channels using a uniform emissivity set to 1, and the actual radiometric temperature was assumed to be equal to the highest computed temperature. Pre-processing of ASTER-derived radiometric temperature consisted of (i) registering the image with an accuracy better than 90 m from reference points (ii) extracting data over three 12 km by 12 km areas centered over the three 9 km^2 sampling areas, (iii) removing data that were visually identified as cloud or as cloud shade on the ground (note that the scene was cloud free over the three 9 km^2 sampling areas Y2, Y9 and Y12) and (iv) re-sampling data at 100 m resolution. An important point is that ASTER-derived radiometric surface temperature was not corrected for atmospheric effects.

The rationale is that only the spatial variability of surface temperature (about the mean) is used by the thermal-based disaggregation algorithm of Merlin et al. (2008a). In other words, there is no need for absolute values of surface temperature. Moreover, atmospheric corrections are generally made at a scale of several tens of kilometers (Thome et al., 1998), which is larger than the application scale (12 km in this study). Similar pre-processing was done on 15 m resolution ASTER red and near-infrared reflectances to derive 100 m resolution NDVI over the three 12 km by 12 km areas.

3. Towards an optimal downscaling resolution

The trade-off between downscaling resolution and accuracy within a disaggregation framework was already mentioned in a previous study (Merlin et al., 2008a). However, Merlin et al. (2008a) did not apply the downscaling approach at multiple resolutions. One objective of this paper is to identify the optimal downscaling resolution(s) in terms of disaggregation accuracy when using data from three sensors: MODIS aboard Terra, MODIS aboard Aqua and ASTER.

3.1. Approach

The approach adopted is to (i) aggregate reference (either PLMR-derived or HDAS-measured) soil moisture to the maximum spatial extent (40 km by 60 km for PLMR and 3 km by 3 km for HDAS), (ii) apply the disaggregation method at a range of resolutions, and (iii) compare the disaggregated soil moisture to the reference data for each downscaling resolution. The disaggregation of soil moisture thus requires simultaneous observations of surface temperature and NDVI. Moreover, validation requires soil moisture observations at a common spatial resolution. Among the twelve dates with at least one (either Terra or Aqua) MODIS image with 0% cloud cover, seven are concurrent with PLMR 1 km resolution flights. For the other five dates (6, 8, 10, 11 and 17 November), the PLMR-derived soil moisture data of the day before are used. This extrapolation is valid because no rainfall occurred between the PLMR flight and MODIS overpass on each date. Data are listed in Table 1. Data derived from MODIS, PLMR, ASTER and HDAS are then aggregated to a range of spatial resolutions. MODIS surface temperature, MODIS NDVI and PLMR soil moisture are aggregated successively from 1 to 12 km in 1 km increments over the 40 km by 60 km area. Similarly, ASTER surface temperature, ASTER NDVI and HDAS soil moisture are aggregated successively from 100 to 1200 m in 100 m increments over the three 9 km^2 sampling areas. One should note that the spacing between ground measurements (250 m) was smaller than the two first aggregation resolutions (100 and 200 m). For these two resolutions, the pixels including no ground measurement were discarded from the analysis and only pixels immediately over the ground measurement sites included. For simplicity, the different spatial resolutions will be denoted using the subscript n, varying from 1 (native resolution) to 12 (for instance, $SM_{PLMR,4}$ refers to PLMR-derived soil moisture aggregated at 4 km resolution and $SM_{mHDAS,5}$ refers to HDAS-measured soil moisture aggregated at 500 m resolution).

3.2. Disaggregation method

The thermal-based disaggregation approach used in this paper is that developed in Merlin et al. (2008a). The equations below represent the case of disaggregation using MODIS data for SMOS-resolution pixels simulated by aggregating PLMR-derived soil moisture. Note that all equations also apply for disaggregation using ASTER data.

The soil moisture $SM_{MODIS,n}$ disaggregated at n km resolution at first order around the SMOS-resolution soil moisture $SM_{PLMR,40}$ is written as

$$SM_{MODIS,n} = SM_{PLMR,40} + \frac{\partial SM}{\partial SEE} \Delta SEE_{MODIS,n} \qquad (1)$$

with $\partial SM / \partial SEE$ being the partial derivative (evaluated at $SM_{SMOS,40}$) of soil moisture to soil evaporative efficiency (SEE), and ΔSEE_n the difference between the MODIS-derived SEE estimated at n km resolution and its average within the SMOS pixel. Eq. (1) can be further simplified by using the simple expression of SEE from Komatsu (2003). The downscaling relationship becomes

$$SM_{MODIS,n} = SM_{PLMR,40} + SM_C \times SMP_{MODIS,n} \qquad (2)$$

with SM_C being a semi-empirical parameter that depends on soil type and boundary layer conditions and SMP a normalized soil moisture proxy. In Merlin et al. (2008a), the SMP was defined as

$$SMP_{MODIS,n} = \frac{T_{MODIS,40} - T_{MODIS,n}}{T_{MODIS,40} - T_{min,1}} \qquad (3)$$

with $T_{MODIS,n}$ being the soil temperature estimated using MODIS-derived NDVI and surface temperature, $T_{MODIS,40}$ its average within the SMOS pixel, and $T_{min,1}$ the minimum MODIS-derived soil temperature at 1 km resolution. Note that the minimum soil temperature was approximated to the minimum MODIS surface temperature. In Komatsu (2003), the parameter SM_C was calibrated for three different soils as function of wind speed

$$SM_C = SM_{C0}\left(1 + \frac{\gamma}{r_{ah}}\right) \qquad (4)$$

with SM_{C0} (vol./vol.) being a soil-dependent parameter (ranging from about 0.01 vol./vol. for sand to 0.04 vol./vol. for clay), and r_{ah} (s m^{-1}) the aerodynamic resistance over bare soil. Aerodynamic resistance can be estimated from wind speed measurements u (m s^{-1}) at reference height Z (m) given the soil roughness z_{0m} (m)

$$r_{ah} = \frac{1}{k^2 u}\left[ln\left(\frac{Z}{z_{0m}}\right)\right]^2 \qquad (5)$$

with k being the von Karman constant. The soil temperature in Eq. (3) is estimated as

$$T_{MODIS,n} = \frac{T_{surf,MODIS,n} - f_{v,MODIS,n} T_{v,n}}{1 - f_{v,MODIS,n}} \qquad (6)$$

with $T_{surf,MODIS,n}$ being the MODIS-derived surface temperature, $T_{v,n}$ the vegetation temperature, and $f_{v,MODIS,n}$ the fractional vegetation cover. In Merlin et al. (2008a), the vegetation temperature was approximated to

Table 1
List of acquisition dates, mean PLMR-derived soil moisture, wind speed measured at Terra (T) or Aqua (A) overpass time (10:30 am/1:30 pm), and minimum MODIS/Terra, MODIS/Aqua and ASTER surface temperature.

Date	$SM_{PLMR,40}$ vol./vol.	u (m s^{-1}) T	A	$T_{min,1}$ (°C) MODIS/T	MODIS/A	ASTER
31 October	0.046		6.0		36.2	
4 November	0.11		7.6		36.5	
5 November	0.065	5.0		35.0		
6 November	0.065*		7.5		37.6	
7 November	0.043	7.4		33.3		
8 November	0.043*	9.4	6.3	31.7	35.4	
9 November	0.040	10.5	4.1	31.4	37.7	
10 November	0.040*	11.9		36.1		
11 November	0.040*	5.3		36.8		
16 November	0.11	13.0				19.0
17 November	0.11*	4.5	3.6	32.2	36.3	
18 November	0.055	5.1		34.7		

* PLMR data from the day before.

$T_{\min,1}$ by assuming that vegetation was not undergoing water stress, and fractional vegetation cover was estimated as

$$f_{v,\text{MODIS},n} = \frac{\text{NDVI}_{\text{MODIS},n} - \text{NDVI}_{\min}}{\text{NDVI}_{\max} - \text{NDVI}_{\min}} \qquad (7)$$

with $\text{NDVI}_{\min}$ and $\text{NDVI}_{\max}$ being the NDVI value that corresponds to bare soil and fully vegetated pixels respectively.

In this study, parameters SM_{C0}, $\text{NDVI}_{\min}$ and $\text{NDVI}_{\max}$, as well as wind speed (r_{ah}) are assumed to be uniform within the SMOS pixel (model parameters are listed in Table 2). This invariance assumption will be further assessed in view of the disaggregation results obtained at a range of spatial resolutions.

3.3. Downscaling resolution versus disaggregation accuracy

Two different criteria are developed to estimate an optimal downscaling resolution for each of the three sensors. The first criterion denoted C1 is the condition that the disaggregation error evaluated at the downscaling resolution is equal to the observed sub-pixel variability. Intuitively, if the error on disaggregated soil moisture is smaller than the sub-pixel variability, then the downscaling resolution is too coarse to represent the actual variability; and conversely if the error is larger, then the downscaling resolution is too fine. C1 can be formulated as

$$\text{RMSE}_{n,n} = \overline{\text{SD}_{n,1}} \qquad (8)$$

with $\text{RMSE}_{n,n}$ being the root mean square error evaluated at the (n km) disaggregation resolution between disaggregated and PLMR-derived soil moisture, and $\overline{\text{SD}_{n,1}}$ the mean standard deviation of 1 km resolution PLMR-derived soil moisture computed within each n^2 km^2 pixel. The n km resolution error is computed as

$$\text{RMSE}_{n,n} = \left[\frac{1}{N/n^2} \sum (\text{SM}_{\text{MODIS},n} - \text{SM}_{\text{PLMR},n})^2 \right]^{0.5} \qquad (9)$$

with N being the number of 1 km resolution pixels within the 40 km by 60 km study area. The mean sub-pixel variability is computed as

$$\overline{\text{SD}_{n,1}} = \frac{1}{N/n^2} \sum \text{SD}_{n,1} \qquad (10)$$

$$= \frac{1}{N/n^2} \sum \left[\frac{1}{n^2-1} \sum (\text{SM}_{\text{PLMR},n} - \text{SM}_{\text{PLMR},1})^2 \right]^{0.5} \qquad (11)$$

The second criterion denoted C2 is the condition that the error evaluated at the native resolution ($n = 1$) is minimum. In other words, C2 is satisfied when the downscaling resolution makes the disaggregation output the most accurate with respect to the reference soil moisture data obtained at the thermal sensor native resolution. C2 can be formulated as

$$\text{RMSE}_{n,1} = \left[\frac{1}{N} \sum (\text{SM}_{\text{MODIS},n} - \text{SM}_{\text{PLMR},1})^2 \right]^{0.5} \text{ is minimum} \qquad (12)$$

with $\text{RMSE}_{n,1}$ being the root mean square error evaluated at 1 km resolution between the n km resolution disaggregated and 1 km resolution PLMR-derived soil moisture.

The criteria C1 and C2 can be applied to the three farms Y2, Y9 and Y12 by replacing in Eqs. (8) to (12) PLMR and MODIS by HDAS and ASTER respectively.

Table 2
Model parameters.

Parameter	Value	Unit	Source
SM_{C0}	0.04	vol./vol.	Komatsu (2003)
γ	100	s m^{-1}	Komatsu (2003)
z_{0m}	0.005	m	Liu et al. (2007)
$\text{NDVI}_{\min}$	0	–	Agam et al. (2007)
$\text{NDVI}_{\max}$	1	–	Agam et al. (2007)

3.4. Application to MODIS

The disaggregation algorithm of Eq. (2) is applied to each of the eight MODIS/Terra images (5, 7, 8, 9, 10, 11, 17 and 18 November) and to each of the six MODIS/Aqua images (31 October, 4, 6, 8, 9 and 17 November), with a downscaling resolution ranging from 1 to 12 km. Fig. 1 plots the n km resolution disaggregated soil moisture versus the n km resolution PLMR-derived soil moisture for $n = 1, 2, 4, 8$ and 12. It is apparent that the noise on disaggregated soil moisture is successively reduced by increasing the downscaling resolution. However, the range of soil moisture values is also reduced and consequently the larger the resolution, the more limited the spatial representation of the actual soil moisture heterogeneity is.

As MODIS data were used for the PLMR soil moisture inversion, PLMR-derived and MODIS-disaggregated soil moisture are theoretically not fully independent on clear sky days. However, it is argued that the cross-correlation of errors in the PLMR soil moisture measurements and the disaggregated soil moisture fields is not responsible for the good results in Fig. 1. One simple reason is that MODIS temperature has a positive impact on PLMR soil moisture retrievals (increasing with MODIS temperature) and a negative impact on disaggregated soil moisture (decreasing with MODIS temperature). Consequently, the cross-correlation of errors in PLMR-derived and MODIS-disaggregated soil moisture would actually make the results poorer.

Fig. 2 plots the $\text{RMSE}_{n,n}$ evaluated at the downscaling resolution as a function of n for each MODIS overpass date, separated according to Aqua and Terra data. The average for all dates is also plotted for each platform. The mean error decreases from about 0.045 vol./vol. at 1 km resolution to about 0.015 vol./vol. at 12 km resolution for both Aqua and Terra. On the same graph is plotted the mean sub-pixel variability $\overline{\text{SD}_{n,1}}$ for all dates. The mean sub-pixel variability increases from 0 to about 0.04 vol./vol. at 1 and 12 km resolution respectively for both Aqua and Terra. The standard deviation is equal to 0 at 1 km resolution because only one PLMR measurement is available per downscaled pixel at 1 km resolution. Following criterion C1 in Eq. (8), an optimal downscaling resolution exists where the RMSE and spatial variability lines cross. Inspection of Fig. 2 shows that the mean optimal resolution is about 3.7 km for MODIS aboard Aqua and 4.2 km for MODIS aboard Terra. Although relatively similar for both sensors, the RMSE of disaggregated soil moisture are remarkably more spread about the mean for Terra than for Aqua. The more consistent disaggregation results using MODIS/Aqua compared to MODIS/Terra was already mentioned in (Merlin et al., 2008a) when applied to 10 km resolution. This is due to the stronger coupling between SEE and soil moisture at 1:30 pm than at 10:30 am.

Fig. 3 plots the average and standard deviation of the error $\text{RMSE}_{n,1}$ (evaluated at the thermal sensor native resolution) as a function n for Aqua and Terra data. The mean error is higher for Terra than for Aqua, which is consistent with previous results. For both Terra and Aqua, the mean error slightly decreases as spatial resolution increases from 1 to 5 km, and slightly increases for spatial resolutions greater than 5 km. Following criterion C2, an optimal downscaling resolution is identified at about 5 km for both MODIS/Terra and MODIS/Aqua. Nevertheless, the minimum of $\text{RMSE}_{n,1}$ is not very well defined since the dynamics of the mean value are smaller than the variability observed within the
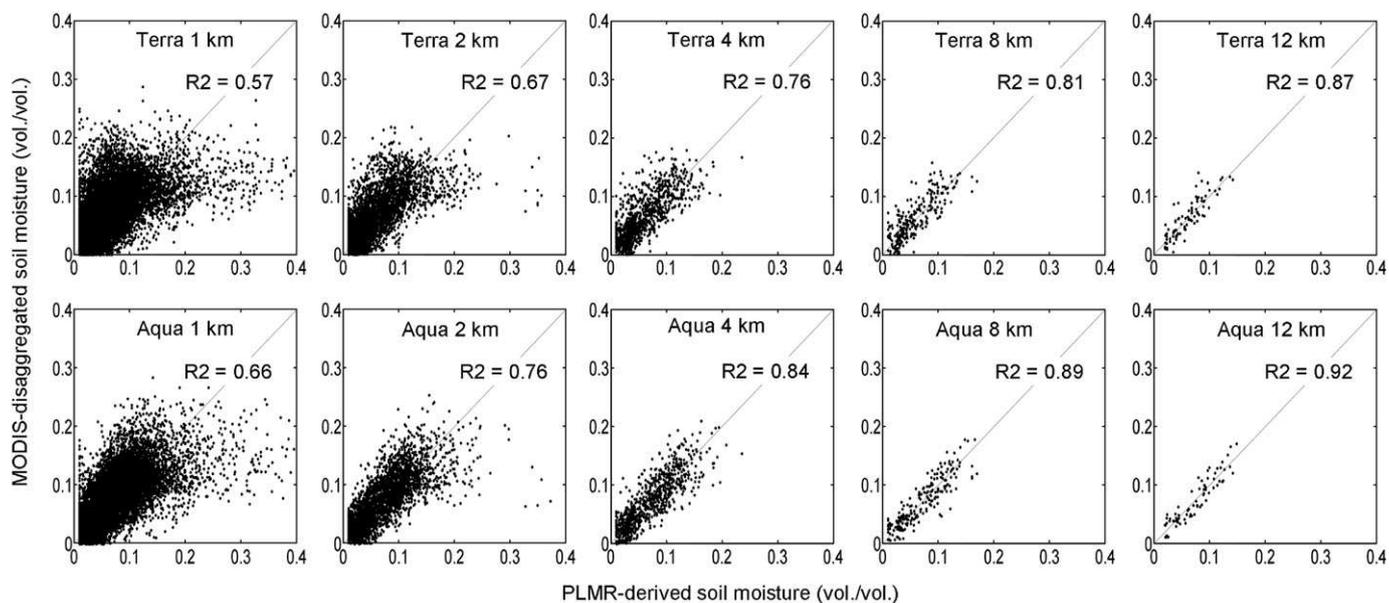
Fig. 1. Scatterplots of the MODIS-disaggregated versus PLMR-derived soil moisture using all twelve days of data for different downscaling resolutions: 1 km, 2 km, 4 km, 8 km and 12 km. The correlation coefficient R2 is indicated on each plot.

data set (shown on Fig. 3 by the standard deviation σ). One limitation of the criterion C2 is that it includes both the uncertainty in the disaggregation output and the uncertainty in PLMR-derived soil moisture at the observation scale, so that the $RMSE_{n,1}$ can never be lower than the measurement error at the native resolution.

In summary, the application of criteria C1 and C2 to MODIS/PLMR data demonstrates that the optimal downscaling resolution in terms of disaggregation accuracy (using the NAFE'06 data set) is about 4 to 5 km. Also, criterion C1 is better defined than C2 since it smooths out the uncertainties associated with random errors in PLMR-derived soil moisture.
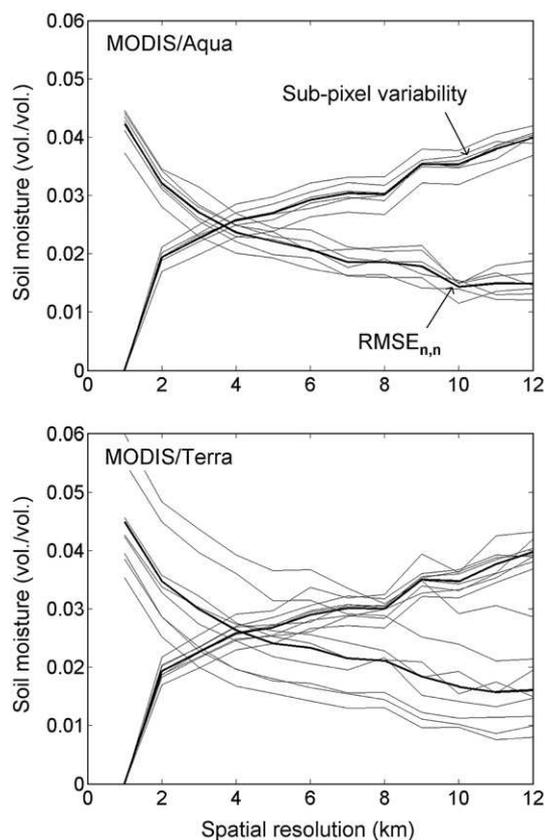

Fig. 2. Estimating an optimal downscaling resolution by comparing the root mean square error (RMSE) and the sub-pixel soil moisture variability at the disaggregation scale. The mean (thick line) RMSE is equal to the mean sub-pixel variability at about 4 km for both MODIS/Aqua and MODIS/Terra. The other lines represent the different dates.
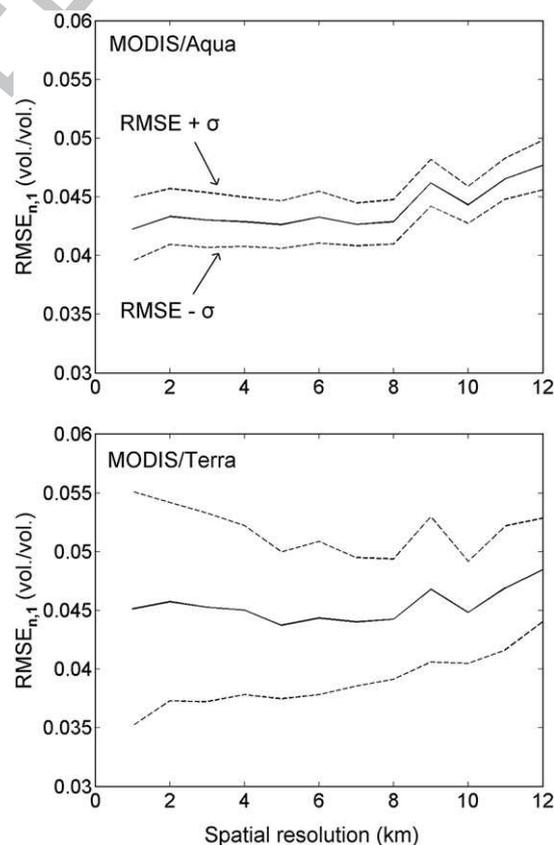

Fig. 3. Root mean square error (RMSE) evaluated at 1 km resolution for downscaling resolutions increasing from 1 to 12 km. Although the standard deviation (σ) between dates is high, the RMSE is minimum at 5 km for both MODIS aboard Aqua and MODIS aboard Terra.

3.5. Application to ASTER

The same disaggregation approach is applied to the three 9 km^2 sampling areas (Y2, Y9 and Y12) using the ASTER/HDAS data collected on 16 November, with a downscaling resolution ranging from 100 to 1200 m. Fig. 4 plots the $n \times 100$ m resolution disaggregated soil moisture versus the $n \times 100$ m resolution aggregated HDAS measurements for $n = 1, 2, 4, 5, 8$ and 12. As with MODIS/PLMR data, it is apparent that the accuracy on disaggregated soil moisture increases (and the range of downscaled values decreases) as the downscaling resolution increases. In Fig. 4, three data points are clearly aside from the 1:1 line for downscaling resolutions of 100 m and 200 m. These correspond to the pixels that included a portion of rice field in Y9. Since rice crops were flooded during NAFE'06, no HDAS measurement was made. Consequently, the nearby ground measurements did not represent well the overall "wetness" (including both soil moisture and standing water) of the surface that the disaggregation algorithm actually represents.

When comparing Figs. 1 and 4, one observes that the disaggregation approach is much more accurate when applied to MODIS data than when applied to ASTER data. In particular for $n = 8$, the correlation coefficient is about 0.80 for MODIS and 0.60 for ASTER. The relatively poor results obtained using ASTER data can be interpreted as a consequence of the spatial variability of soil moisture at fine scale. As the typical crop size in the study area was about 100–300 m, soil moisture fields were much more heterogeneous at 100 m resolution than at 1 km and above. It is suggested that point-scale measurements aggregated at 100–1000 m resolution were generally more uncertain than 1 km resolution remotely-sensed PLMR-derived soil moisture.

Fig. 5 plots the RMSE$_{n,n}$ evaluated at the downscaling resolution as a function of n. It is apparent that the error is approximately constant at 100 m and 200 m resolution, which is consistent with the fact that the spacing (250 m) of HDAS measurements was larger than the thermal sensor native resolution so that the spatial variability of HDAS measurements is not represented below 300 m. For all farms, the error is maximum at 200 m, and is minimum at 1200 m resolution with a value of about 0.02 vol./vol. On the same graph is plotted the mean sub-pixel variability $\overline{SD}_{n,1}$ for each farm. The mean variability is about 0.02 vol./vol. at $n = 1$ and is generally maximum at $n = 12$. Note that
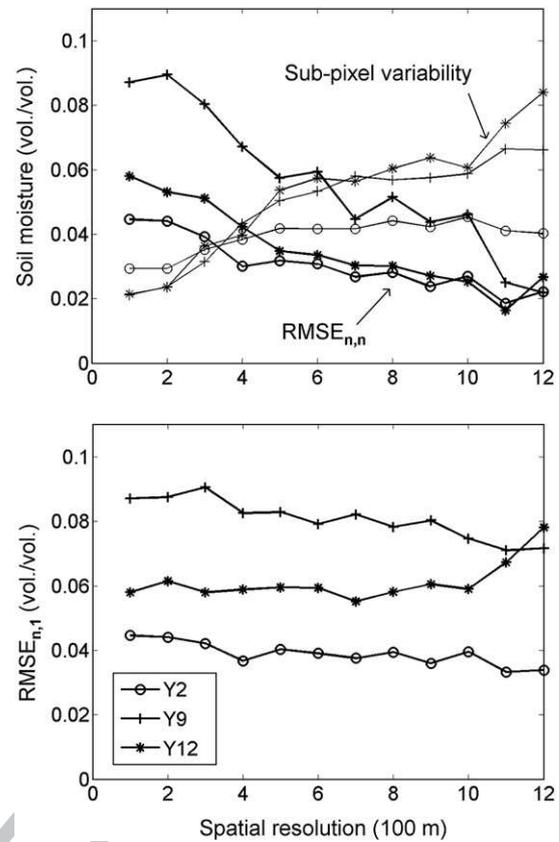

Fig. 5. Root mean square error (RMSE) evaluated at the downscaling resolution (top) and at 100 m resolution (bottom) for downscaling resolutions increasing from 100 to 1200 m.

its value at $n = 1$ is not equal to zero as in the case of PLMR data, because three successive measurements were made at each sampling point, providing the mean local-scale variability of HDAS measurements. Following criterion C1 in Eq. (8), the optimal downscaling resolution for each farm is identified at 300 m, 400 m and 600 m for Y2, Y9 and Y12 respectively.
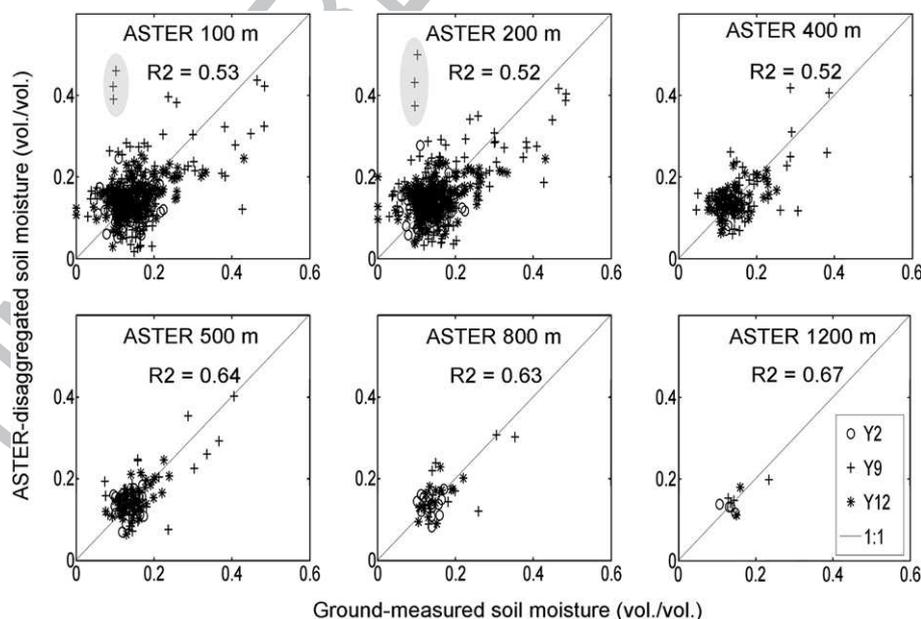

Fig. 4. Scatterplots of the ASTER-disaggregated versus ground-measured soil moisture on 16 November for different downscaling resolutions: 100 m, 200 m, 400 m, 500 m, 800 m and 1200 m. Highlighted pluses correspond to pixels containing standing water (flooded rice fields). The correlation coefficient R2 is indicated on each plot.

Fig. 5 also plots the error $RMSE_{n,1}$ evaluated at the ASTER native resolution (100 m) as a function of n. Although one observes a minimum of the error for Y12 at $n = 7$, no minimum is observed for the other farms (Y2 and Y9). Several hypotheses can be postulated to explain these constrasting results. First, when using ground measurements instead of airborne L-band data, reference soil moisture data are representative of the point-scale and may not be representative of the scales integrated to several hundreds of meters, especially over highly heterogeneous irrigated areas like in Y9. Second, the farm-scale variability in Y2 was about the same as the local-scale variability (uncertainty in a single HDAS measurement). Consequently, the disaggregation over that farm was not expected to improve the accuracy of soil moisture at fine scale. Third, it was seen in the case of MODIS/PLMR that criterion C2 was not very stable from date to date, so no clear result can be expected from only one date with ASTER/HDAS.

In summary, the application of criteria C1 and C2 to ASTER/HDAS data suggests that the optimal downscaling resolution in terms of disaggregation accuracy (using the NAFE'06 data set) is about 4 to 5 times the thermal sensor resolution. Criterion C1 is again found to be better defined than C2.

4. Sequential disaggregation

The general approach of the sequential disaggregation using multi-resolution thermal sensors is presented in Fig. 6. The ~40 km resolution SMOS-scale soil moisture generated from PLMR data on 16 November is disaggregated at an intermediate resolution (4 km in Fig. 6) using MODIS data and the MODIS-disaggregated soil moisture is disaggregated again at a finer resolution using ASTER data. Note that the MODIS data on 16 November were not cloud free over the 40 km SMOS-scale pixel so that the MODIS data on 17 November were used instead.

4.1. A sequential model

The sequential model is written as

$$SM_{S_{i+1}} = SM_{S_i} + \frac{\partial SM}{\partial SEE} \Delta SEE_{S_{i+1}} \tag{13}$$

with S_i being the sensor of index i. In our case, S_0, S_1 and S_2 corresponds to SMOS, MODIS and ASTER respectively. By using this notation, Eqs. (2) and (3) become

$$SM_{S_{i+1}} = SM_{S_i} + SM_C \times SMP_{S_{i+1}} \tag{14}$$

with

$$SMP_{S_{i+1}} = \frac{T_{S_i} - T_{S_{i+1}}}{T_{S_i} - T_{min}} \tag{15}$$

From the above equations, one is able to identify the parameters that do not vary with scale. In particular, the minimum soil temperature
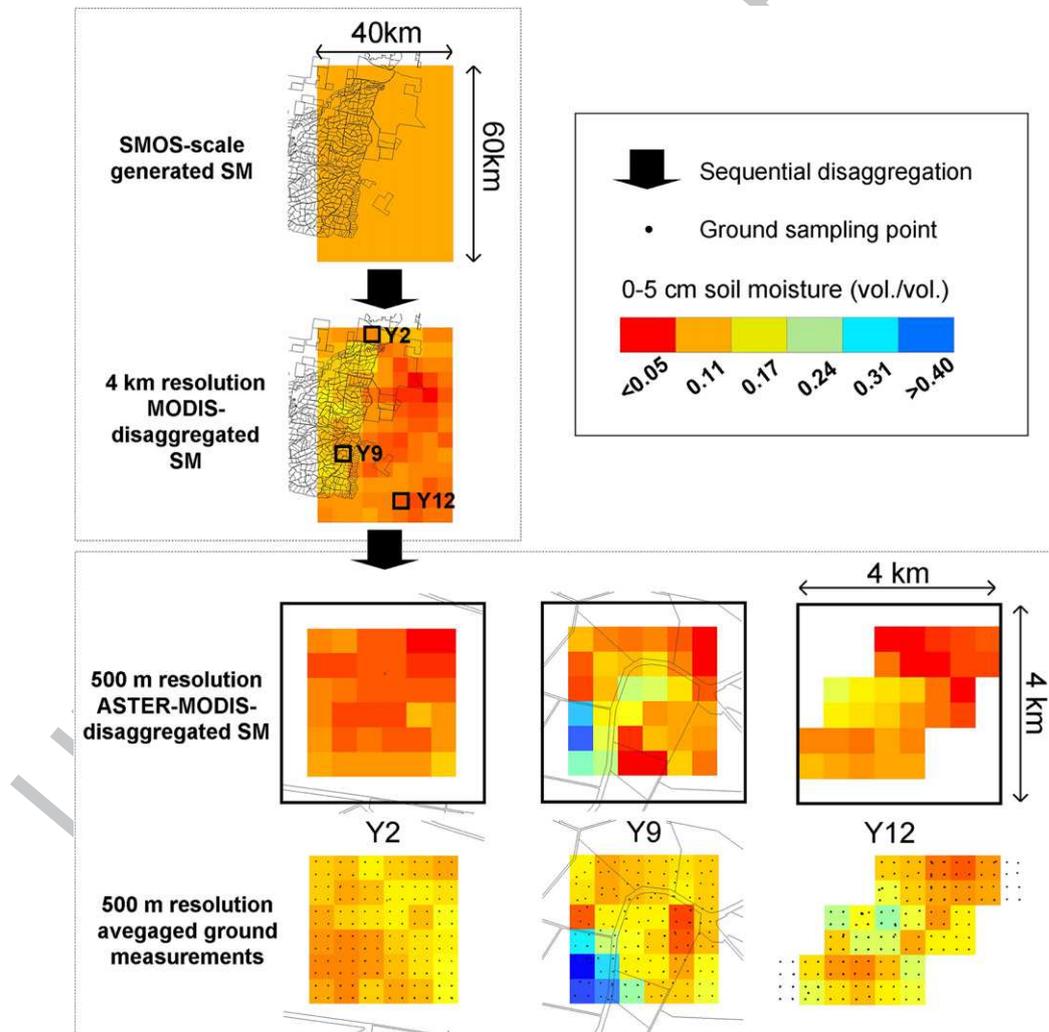

Fig. 6. Schematic diagram presenting the sequential disaggregation of SMOS-scale soil moisture using MODIS and ASTER data.

T_{min} and the soil property SM_C are assumed to be scale-invariant. An important point is that these assumptions might not be valid in the case of heterogeneous soil within the SMOS-scale pixel. In particular, Merlin et al. (2008a) demonstrated that estimating SM_C at high resolution improved significantly the disaggregation accuracy. However, the scale-invariance of SM_C was not tested in this paper since only one ASTER image was available whereas a time series would be required (Merlin et al., 2008a).

4.2. Application

Based on the results of the previous section, the intermediate resolution is set to four times the MODIS native resolution (4 km) and the target resolution to five times the ASTER native resolution (500 m). In practice, three data sets were derived by defining a 4 km resolution pixel centered on each of the three sampling areas (see black outlines in Fig. 6). This pixel was used to create over the SMOS-scale pixel a 4 km resolution grid, on which the 1 km resolution MODIS and PLMR data were aggregated. The sequential model of Eq. (14) was finally applied to each data set.

Fig. 7 plots the 4 km resolution MODIS-disaggregated soil moisture versus the 4 km resolution PLMR-derived soil moisture for each of the three data sets. The root mean square error is 0.026 vol./vol. Fig. 7 also plots the 500 m resolution ASTER-MODIS-disaggregated soil moisture versus the 500 m resolution HDAS-measured soil moisture in each farm. The sequentially disaggregated soil moisture has a RMSE of 0.062 vol./vol. and a bias of −0.045 vol./vol. Results are degraded compared to the case when the ASTER-disaggregated soil moisture was based on HDAS-aggregated measurements and not on MODIS-disaggregated soil moisture. The increase of uncertainty could be due

Fig. 8. Scatterplots of the 1 km resolution ASTER-MODIS-disaggregated soil moisture versus HDAS measurements for three different intermediate resolutions: 4 km, 8 km and 12 km, and for the case of "no intermediate resolution".

to the disaggregation method and/or the soil moisture retrieval algorithm. The bias on disaggregated soil moisture is estimated as −0.047, −0.040 and −0.049 vol./vol. for Y2, Y9 and Y12 respectively. Although a persistent bias of about −0.045 vol./vol. tends to corroborate the hypothesis of a bias in the PLMR-derived soil moisture on 16 November, no conclusion can be drawn from only three independent data sets.

Errors on disaggregated soil moisture might also come from the disaggregation method itself, which may not fully represent the non-linear behaviour of the relationship between SEE and soil moisture. The effect of this non-linearity is clearly visible in Fig 7 where MODIS-disaggregated soil moisture tends to saturate at PLMR-derived soil moisture values higher than 0.20 vol./vol. Moreover, our sequential model did not account for the propagation of errors in the disaggregation. In particular, a random error in MODIS-disaggregated soil moisture at 4 km resolution would behave as a bias on 500 m resolution ASTER-MODIS-disaggregated soil moisture within each 4 km resolution pixel.

One way to limit the increase of uncertainty associated with error propagations would be to choose a coarser target resolution. In
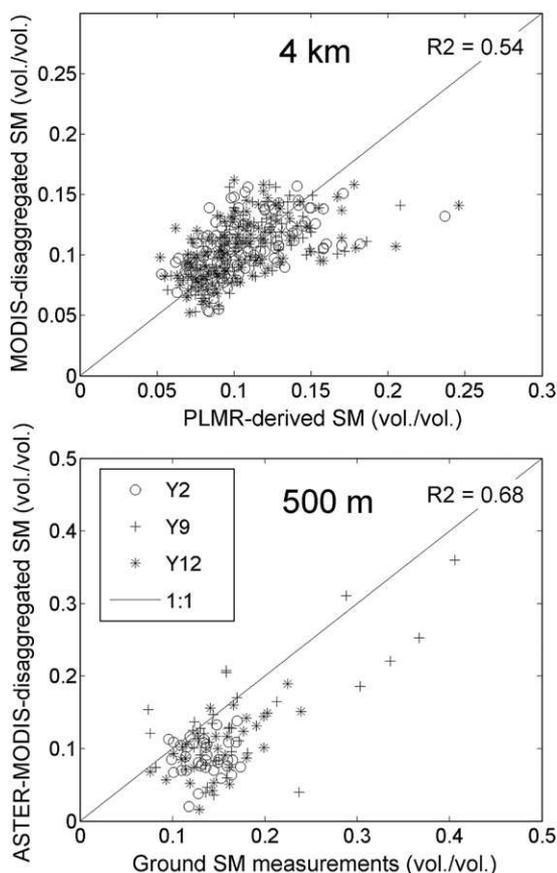

Fig. 7. Scatterplots of the 4 km resolution MODIS-disaggregated versus 4 km aggregated PLMR-derived soil moisture (top) and the 500 m resolution ASTER-MODIS-disaggregated versus 500 m HDAS measurements (bottom).
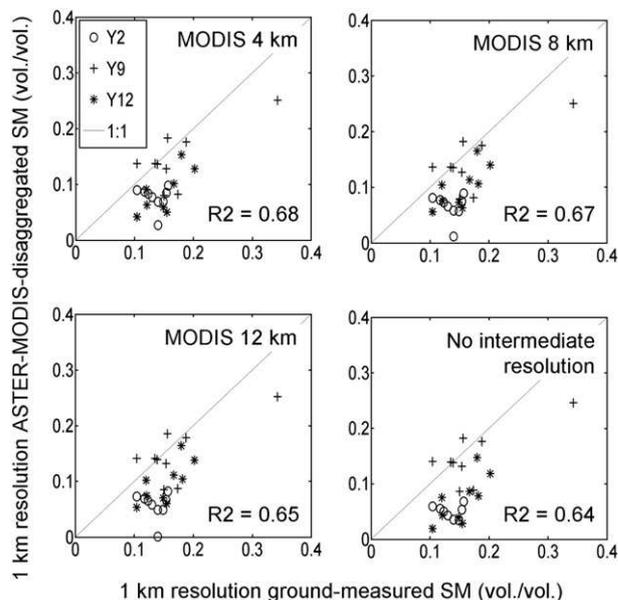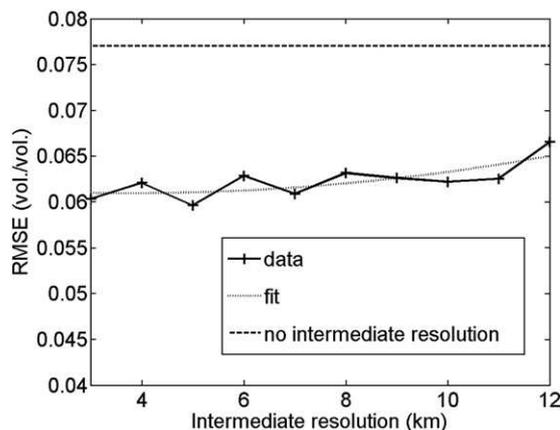

Fig. 9. Root mean square error on the 1 km resolution ASTER-MODIS-disaggregated soil moisture for an intermediate resolution increasing from 3 to 12 km. The error obtained in the case of "no intermediate resolution" is also indicated.

particular, output errors are expected to be reduced by setting the downscaling resolution to a value larger than the resolution that was found to be optimal when using one sensor (MODIS or ASTER) independently from the combination of both.

4.3. Sensitivity to intermediate resolution

Due to propagation errors from the coarser to finer resolutions, the combination of multi-source (MODIS and ASTER) data is likely to increase the disaggregation uncertainty. Consequently, one may argue that a more efficient approach than combining MODIS and ASTER data would be the direct disaggregation of SMOS-scale soil moisture using ASTER data only. The point is the swath width of ASTER (60 km) is much narrower than that of SMOS (~1000 km). In particular, the 40 km by 60 km area covered by PLMR (SMOS-scale pixel) during NAFE'06 was not entirely covered by ASTER. Therefore, the disaggregation of SMOS-scale soil moisture requires thermal data at an intermediate resolution (MODIS) before the use of high-resolution (ASTER) data over smaller focus areas.

To assess the sensitivity of disaggregation results to intermediate resolution, an additional analysis is presented. The target resolution is now fixed to 1 km, and the intermediate resolution is increased from 3 to 12 km in 1 km increments. The 1 km resolution ASTER-MODIS-disaggregated soil moisture is then compared to ground measurements aggregated at 1 km resolution. Pre-processing included (i) defining a pixel with a resolution ranging from 3 to 12 km and covering each of the three 9 km^2 sampling areas (ii) creating a 3–12 km resolution grid over the SMOS-scale pixel based on that pre-defined pixel and (iii) aggregating 1 km resolution MODIS and PLMR data at 3–12 km resolution on that pre-defined grid. The sequential model of Eq. (14) was finally applied to each data set for an intermediate resolution ranging from 3 to 12 km.

Fig. 8 plots the 1 km resolution ASTER-MODIS-disaggregated versus HDAS-measured soil moisture for three different intermediate resolutions: 4, 8 and 12 km and for the case of "no intermediate resolution". For the case "no intermediate resolution", the SMOS pixel is disaggregated at 1 km resolution directly using only the ASTER data. As the ASTER image did not entirely cover the SMOS pixel, the mean temperature required in Eq. (15) was estimated within the overlap area of ASTER and PLMR data, which represented about 80% of the SMOS pixel. The RMSE on sequentially disaggregated soil moisture is 0.060 and 0.077 vol./vol., the bias − 0.049 and − 0.063 vol./vol., and the correlation coefficient 0.68 and 0.64 at 4 km and ~40 km resolution respectively. The error is plotted as a function of intermediate resolution in Fig. 9. It is apparent that the error is minimum at 3–5 km and slightly increases with intermediate resolution, meaning that the optimal intermediate resolution is the highest. Note that the oscillation of the RMSE around its upward trend is mainly due to the change of the spatial extent of input data each time data are aggregated to a different intermediate resolution. For intermediate resolutions ranging from 3 to 12 km, the error is lower than that obtained in the case of "no intermediate resolution". This shows that the use of MODIS data in the sequential disaggregation increases the accuracy on ASTER-disaggregated soil moisture. It is suggested that the use of an intermediate resolution between SMOS and ASTER is able to reduce the non-linearity effects across scales between soil evaporative efficiency and soil moisture, despite the increase of uncertainties associated with error propagations.

5. Conclusion

A sequential model was developed to disaggregate microwave-derived soil moisture recursively from 40 km to 4 km resolution using MODIS data and from 4 km to 500 m resolution using ASTER data. The airborne and ground data collected during the three-week NAFE'06 were used to simulate coarse-scale pixels, and a thermal-based disaggregation algorithm was applied using 1 km resolution MODIS and 100 m resolution ASTER data. A key step in the procedure was to identify an optimal downscaling resolution in terms of disaggregation accuracy and sub-pixel soil moisture variability by using two criteria. The first criterion C1 was to look for the spatial resolution such that the RMSE evaluated at the downscaling resolution be equal to the sub-pixel soil moisture variability, while the second criterion C2 was to look for the spatial resolution that minimized the RMSE evaluated at the thermal sensor native resolution (1 km for MODIS or 100 m for ASTER). Very consistent optimal downscaling resolutions were obtained for MODIS aboard Terra, MODIS aboard Aqua and ASTER, which were 4 to 5 times the thermal sensor resolution.

The ~40 km resolution SMOS-scale soil moisture generated from airborne L-band data on 16 November was disaggregated at an intermediate resolution (4 km) using MODIS data and the MODIS-disaggregated soil moisture was disaggregated again at 500 m resolution using ASTER data. The RMSE between the 500 m resolution sequentially-disaggregated and ground-measured soil moisture was 0.062 vol./vol. with a bias of − 0.045 vol./vol. and soil moisture values ranging from 0.08 to 0.40 vol./vol. To assess the impact of the intermediate resolution on disaggregation accuracy, a different approach was proposed by setting the target resolution to 1 km and by increasing the intermediate resolution from 3 to 12 km. The optimal intermediate resolution was found to be 3–5 km, meaning that the use of MODIS data reduced the non-linearity effects across scales between SMOS and ASTER resolutions, despite the increase of uncertainties associated with the combination of MODIS and ASTER data.

Beyond the application of multi-resolution soil moisture data to a range of environmental sciences, such an approach could greatly facilitate the validation of coarse-scale microwave-derived soil moisture data using point-scale ground measurements. The sequential model is being implemented over the Valencia Anchor Station area (Lopez-Baeza et al., 2007) in the SMOS calibration/validation framework.

Note that the operational application of thermal-based methods would require high-spatial-resolution thermal data acquired at high-temporal-resolution, typically 2–3 days. However, high-spatial-resolution (ASTER-like) thermal data are currently available on a monthly basis, which raises the issue of disaggregating low-spatial-resolution (MODIS-like) thermal data at high-temporal-resolution (Agam et al., 2007).

Refinements of the sequential disaggregation method would include a physical calibration of the soil evaporative efficiency model, which is at present semi-empirical. Moreover, the disaggregation accuracy is affected by the non-linearity of that exponential function. Recent developments have accounted for the non-linearity of the models used in the disaggregation of remote sensing data with the projection technique (Merlin et al., 2006) or the Taylor series including derivative terms at orders superior to 1 citepmerlin08c. The applicability of those approaches and their stability still need to be confirmed at a range of spatial resolutions.

References

Agam, N., Kustas, W. P., Anderson, M. C., Li, F., & Neale, C. M. U. (2007). A vegetation index based technique for spatial sharpening of thermal imagery. *Remote Sensing of Environment*, *107*, 545–558.

Bindlish, R., & Barros, A. P. (2002). Subpixel variability of remotely sensed soil moisture: An inter-comparison study of SAR and ESTAR. *IEEE Transactions on Geoscience and Remote Sensing*, *40*, 326–337.

Chehbouni, A., Escadafal, R., Duchemin, B., Boulet, G., Simonneaux, V., Dedieu, G., Mougenot, B., Khabba, S., Kharrou, H., Maisongrande, P., Merlin, O., Chaponnière, A., Ezzahar, J., Er-Raki, S., Hoedjes, J., Hadria, R., Abourida, A., Cheggour, A., Raibi, F., Boudhar, A., Benhadj, I., Hanich, L., Benkaddour, A., Guemouria, N., Chehbouni, A. H., Lahrouni, A., Olioso, A., Jacob, F., Williams, D. G., & Sobrino, J. A. (2008). An integrated modelling and remote sensing approach for hydrological study in arid and semi-arid regions: The SUDMED Programme. *International Journal of Remote Sensing*, *29*(17), 5161–5181.

Choudhury, B. J. (1994). Synergism of multispectral satellite observations for estimating regional land surface evaporation. *Remote Sensing of Environment*, *49*(3), 264–274.

Crow, W. T., Ryu, D., & Famiglietti, J. S. (2005). Upscaling of field-scale soil moisture measurements using distributed land surface modeling. *Advances in Water Resources*, *28*(1), 1–14.

Das, N. N., & Mohanty, B. P. (2008). Temporal dynamics of PSR-based soil moisture across spatial scales in an agricultural landscape during SMEX02: A wavelet approach. *Remote Sensing of Environment*, *112*, 522–534.

Dubayah, R., Wood, E. F., & Lavallee, D. (1997). Multiscaling analysis in distributed modeling and remote sensing: An application using soil moisture. In D. A. Quattrocchi, & M. Goodchild (Eds.), *Scale in Remote Sensing and GIS* New York: Lewis Publisher.

Gillespie, A. R. (1985). Lithologic mapping of silicate rocks using TIMS. *The TIMS Data User's Workshop* (pp. 29–44). Pasadena, CA: JPL pub Vol. 86–38.

Kerr, Y. H., Waldteufel, P., Wigneron, J. -P., Martinuzzi, J. -M., Font, J., & Berger, M. (2001). Soil moisture retrieval from space: The soil moisture and ocean salinity (SMOS) mission. *IEEE Transactions on Geoscience and Remote Sensing*, *39*, 1729–1735.

Kim, G., & Barros, A. P. (2002). Downscaling of remotely sensed soil moisture with a modified fractal interpolation method using contraction mapping and ancillary data. *Remote Sensing of Environment*, *83*, 400–413.

Kim, G., & Barros, A. P. (2002). Space-time characterization of soil moisture from passive microwave remotely sensed imagery and ancillary data. *Remote Sensing of Environment*, *81*, 393–403.

Komatsu, T. S. (2003). Towards a robust phenomenological expression of evaporation efficiency for unsaturated soil surfaces. *Journal of Applied Meteorology*, *42*, 1330–1334.

Liu, S., Mao, D., & Jia, L. (2007). Evaluating parameterizations of aerodynamic resistance to heat transfer using field measurements. *Hydrology and Earth System Science*, *11*, 769–783.

Lopez-Baeza, E., Vidal, S., Cano, A., Domenech, C., Geraldo-Ferreira, A., Millan-Scheiding, C., Narbon, C., Sanchis, J., & Velazquez, A. (2007). Representativity of the Valencia and the Alacant anchor stations in the context of validation of remote sensing algorithms and low-resolution products. *Proceedings of the Joint 2007 EUMETSAT Meteorological Satellite Conference and the 15th Satellite Meteorology and Oceanography Conference of the American Meteorological Society. Amsterdam.*

Merlin, O., Chehbouni, G., Kerr, Y., & Goodrich, D. (2006). A downscaling method for distributing surface soil moisture within a microwave pixel: Application to the Monsoon'90 data. *Remote Sensing of Environment*, *101*, 379–389.

Merlin, O., Walker, J. P., Chehbouni, A., & Kerr, Y. (2008). Towards deterministic downscaling of SMOS soil moisture using MODIS derived soil evaporative efficiency. *Remote Sensing of Environment*, *112*, 3935–3946. doi:10.1016/j.rse.2008.06.012.

Merlin, O., Walker, J. P., Kalma, J. D., Kim, E. J., Hacker, J., Panciera, R., Young, R., Summerell, G., Hornbuckle, J., Hafeez, M., & Jackson, T. J. (2008). The NAFE'06 data set: Towards soil moisture retrieval at intermediate resolution. *Advances in Water Resources*, *31*, 1444–1455. doi:10.1016/j.advwatres.2008.01.018.

Merlin, O., Walker, J. P., Panciera, R., Escorihuela, M. J., & Jackson, T. J. (2009). Assessing the SMOS soil moisture retrieval parameters with high-resolution NAFE'06 data. *Geoscience Remote Sensing Letters.* doi:10.1109/LGRS.2008.2012727.   **Q2**

Realmuto, V. J. (1990). Separating the effects of temperature and emissivity: Emissivity spectrum normalization. *2nd TIMS Workshop* (pp. 310–316). Pasadena, CA: JPL pub Vol. 90–55.

Rodriguez-Iturbe, I., Vogel, G. K., & Rigon, R. (1995). On the spatial organization of soil moisture fields. *Geophysical Research Letters*, *22*(20), 2757–2760.

Thome, K., Palluconi, F., Takashima, T., & Masuda, K. (1998). Atmospheric correction of ASTER. *IEEE Transactions on Geoscience and Remote Sensing*, *36*(4), 1199–1211. doi:10.1109/36.701026.

Wan, Z. (2008). New refinements and validation of the MODIS land-surface temperature/emissivity products. *Remote Sensing of Environment*, *112*(1), 59–74. doi:10.1016/j.rse.2006.06.026.

Western, A. W., Grayson, R. B., & Bloschl, G. (2002). Scaling of soil moisture. *Annual Review Earth Planetary Science*, *30*, 149–180.